OPERATIONAL VALIDATION STRATEGIES FOR SATELLITE-BASED SOIL MOISTURE PRODUCTS OVER ARGENTINE PAMPAS

Journal:	*Journal of Selected Topics in Applied Earth Observations and Remote Sensing*
Manuscript ID:	JSTARS-2014-00884
Manuscript type:	vol8_6 IGARSS 14
Date Submitted by the Author:	30-Sep-2014
Complete List of Authors:	Grings, Francisco; Institute of Astronomy and Space Physics (IAFE), Remote Sensing; Institute Of Astronomy and Space Physics, Remote Sensing Bruscantini, Cintia; IAFE, teledetección Smucler, Ezequiel; Institute Of Astronomy and Space Physics, Remote Sensing Carballo, Federico; Institute of Astronomy and Space Physics (IAFE), Remote Sensing; Institute Of Astronomy and Space Physics, Remote Sensing Dillon, Maria Eugenia; Consejo Nacional de Investigaciones Científicas y Técnicas (CONICET) & Servicio Meteorológico nacional (SMN), Remote Sensing Collini, Estela; Servicio de Hidrografia Naval (SHN) & Servicio Meteorológico nacional (SMN), Remote Sensing Salvia, Mercedes; IAFE - Institute for Astronomy and Space Physics, Remote Sensing Group; Karszenbaum, Haydee; Institue of Astronomy and Space Physics (IAFE), Remote Sensing
Keywords:	Remote sensing, Soil measurements, Microwave radiometry

OPERATIONAL VALIDATION STRATEGIES FOR SATELLITE-BASED SOIL MOISTURE PRODUCTS OVER ARGENTINE PAMPAS

Grings, F. (1), Bruscantini, C. (1), Smucler, E. (1), Carballo, F. (1), Dillon, M. E. (2), Collini, E. (3), Salvia, M (1), Karszenbaum, H (1).

(1) Quantitative Remote Sensing Group, Institute of Astronomy and Space Physics (IAFE), University of Buenos Aires, Buenos Aires 1428, Argentina, verderis@iafe.uba.ar,
(2) Consejo Nacional de Investigaciones Científicas y Técnicas (CONICET) & Servicio Meteorológico nacional (SMN)
(3) Servicio de Hidrografia Naval (SHN) & Servicio Meteorológico nacional (SMN)

ABSTRACT

In this paper, an operational evaluation strategy for two candidates satellite derived SM products is presented. In particular, we analyze the performance of two candidate algorithms (SMOS-based SM and ASCAT-based SM) to monitor SM in Pampas Plain. The difficulties associated with commonly used evaluation techniques are addressed, and advanced techniques are presented. In particular, we introduce comparisons with a land surface model (GLDAS) and SM anomalies and Triple Collocation analyses. Then, we discuss the relevance of these analyses in the context of end users requirements, and propose an extreme events-detection analysis based on anomalies of the Standardized Precipitation Index and satellite-based soil moisture anomalies. The results show that: (1) both ASCAT and SMOS spatial anomalies data are able to reproduce the expected SM spatial patterns of the area, (2) both ASCAT and SMOS temporal anomalies are able to follow the measured in situ SM temporal anomalies and (3) both products were able to monitor large Standardized Precipitation Index extremes, at least in conditions where crop biomass was moderate to low.

1. INTRODUCTION

Satellite-based soil moisture (SM) products are potentially useful for several key environmental applications (agro-meteorology, SM excess or deficit monitoring, etc). The information provided by these systems is particularly relevant in Argentina's Pampas Plain, where in situ meteorological stations are scarce and frequent extreme environmental events strongly affect agricultural production.

There are several satellite-based, global, operational SM products available for the Pampas Plain area (e.g. Aquarius, ASCAT, SMOS, AMSR-E). Nevertheless, SM products obtained from these satellite systems report different spatiotemporal patterns of SM for the same area and period of time. These products discrepancy was also observed for other areas around the world, and it is the subject of active research, since all these products claim some form of validation (in general, in situ validation in some densely instrumented sites), and were successfully used in several derived applications (e.g. assimilation in forecast models, SM-precipitation coupling, run-off models). In some way, all existing products could represent “true” SM to some extent.

Therefore, it is relevant to ask which products best reproduce Pampas Plain SM spatiotemporal patterns. This is not an easy question to answer, since there are no validation sites in this area and therefore direct validation is not possible at the time. Therefore, since: (1) product quality in the area cannot be guaranteed by global validation and (2) direct in situ validation is not possible, alternative validation schemes become relevant.

In this paper, we analyze the performance of two candidate algorithms (SMOS-based SM and ASCAT-based SM) to monitor SM in Pampas Plain. The difficulties associated with commonly used evaluation techniques are addressed, and advanced techniques are presented. In particular, we introduce comparisons with a land surface model (GLDAS) and SM anomalies and Triple Collocation (TC) analyses [1]. Then, we discuss the relevance of these analyses in the context of end users requirements, and propose an extreme events-detection analysis based on anomalies of the Standardized Precipitation Index (SPI). Finally, the implications of these results to define site-specific operational evaluation strategies are

discussed. The following sections address these subjects, starting with a short description of the Pampas Plains locations and of the characteristics of the satellite systems products under discussion.

2. THE PAMPAS PLAINS

Argentina's Pampas (27-40º S, 57-67º W) is a wide plain of over 50 million ha of fertile lands suitable for cattle and crop production. Figure 1 show a land cover map of the area [2] and, as an example, the spatial distribution of the difference between precipitation (P) and evapotranspiration (EP) means (mm) of the period 1970-2006 for the month of October (growing season) as a reference of the hydrological characteristics of the area, drier in the west and wetter in the east [3]. Most of the Pampas region is significantly affected by cyclical drought and flood episodes that impact both crop and cattle production.

Figure 1. Study area. (left) Pampas Plains land cover categories (adapted from [2]) and (right) an example of the spatial distribution of the P-EP for the period 1970-2006 for the month of October (adapted from [3]).

3. AVAILABLE DATA

3.1. Satellite data

There are several satellite based soil moisture products available in the study area. For this study, we selected two of them (ASCAT [4] and SMOS [5]) whose overall global performance and popularity makes them candidates to provide a reasonable estimation of SM spatiotemporal distribution in our study area.

The SMOS satellite was launched in 2009 and is dedicated to SM retrieval at ~5 cm depth using brightness temperature measured at L-band (passive microwave). It has a single observation frequency (1.4 GHz), but uses observations at multiple incident angles. The standard SMOS algorithm is based on the L-MEB (L-band Microwave Emission of the Biosphere) model and it adopts a forward modeling approach to solve for SM [5]. However, the algorithm has an additional degree of freedom to accommodate different soil types and land covers. In this paper, we used the SM data set provided by EOLI-SA data source.

The ASCAT sensor onboard the MetOp-A measures the backscattering coefficient at C-band and at multiple incidence angles (active microwave). The SM estimation is obtained using a time-series based change-detection algorithm [4]. Since the SM changes can be measured in relative terms, the estimation becomes less susceptible to the adverse influence of vegetation cover and surface roughness.

3.2. LSM data

Other relevant providers of SM spatiotemporal distribution information are Land Surface Models. These models estimate SM solving the energy/mass balance in the earth surface and constraints its retrieval assimilating in situ data. In order to compare models and product estimations, we included in the analysis the NOAH version of GLDAS. GLDAS soil moisture product is produced by specific instances of the Land Information System (LIS) software framework for high-performance land-surface modeling and data assimilation developed within the Hydrological Sciences Laboratory at NASA Goddard.

In order to quantitatively analyze the data, products were gridded into the GLDAS official grid using nearest neighbor interpolation.

3.3. In situ data

Although no field validation site exists in the study area, there are SM data available, acquired in the SOL NEGRO agricultural site near the city of Cordoba, Argentina. SM was measured using an Hydra Probe II system with a sampling depth of 5 cm every hour since September 2012 [6].

Since point SM measurements provide only limited validation capacity, we estimated soil hydrological condition using the Standardized Precipitation Index (SPI). Therefore, in situ precipitation data were extensively used. Over the area considered, the National Meteorological Service (NMS) of Argentina provides daily precipitation data of approximately 50 ground stations.

4. METHODOLOGY

4.1. Spatial anomalies

As we will see in the following section, a direct comparison between SM products leads to poor results both quantitatively and qualitatively, since it does not allow answering the questions posed in the introduction. Therefore, in order to compare the spatial patterns of the three soil moisture data sets, we generated maps of each of the products' standardized spatial anomalies. For each SM data set standardized spatial anomalies were calculated in three steps, as follows. We first calculated for each grid point in the study region the product's mean. Second, we calculated the spatial mean and standard deviation of the means calculated in the first step. Finally, we defined the standardized spatial anomaly of the given SM data set at a given grid point as the difference between the mean calculated at that grid point in the first step and the spatial mean calculated in the second step, divided by the spatial standard deviation calculated in the second step. These maps provide information on how similarly each of the SM data sets represents wet/dry conditions over the study region. In order to quantify this information, we calculated the linear correlation coefficient between the standardized spatial anomalies of each pair of SM data sets [1].

4.2. Triple Collocation (TC)

The triple collocation (TC) technique, developed by [7], is a tool to estimate the root means squared error (RMSE) with respect to the real in situ variable in remote sensing products. This technique is used here to estimate RMSE of the soil moisture anomalies time series generated by GLDAS (X), SMOS (Y) and ASCAT (Z). The soil moisture temporal anomalies time series were defined as the deviations of the original time series from their seasonal climatology. For each data set, the seasonal climatology was calculated as the 31 day moving average, where the averages are based on data from the whole period of study for the 31 day window surrounding each day of the year.

At each grid point and for each data set, TC adopts the following model to relate the data sets to the (unknown) true soil moisture anomalies (t):

$$X = \beta_X (t + \varepsilon_X) \qquad (1)$$

$$Y = \beta_Y (t + \varepsilon_Y) \qquad (2)$$

$$Z = \beta_Z (t + \varepsilon_Z) \qquad (3)$$

where β_i and ε_i for i = X, Y, Z are the TC calibration constants and errors corresponding to GLDAS , SMOS and ASCAT respectively. The errors ε_i for i = X, Y, Z are assumed to be zero-mean random variables, which are uncorrelated with each other and with the truth (t). The calibration constants are used to rescale the data sets, so as to eliminate systematic differences in their variability. Since equations (1)-(3) are underdetermined, one data set is chosen as the reference and the other two are rescaled to the reference time series. The data set chosen as the reference here is GLDAS. This selection is not arbitrary, since we expect GLDAS to provide the SM benchmark information for the area.

Therefore we set $\beta_X = 1$ and estimate the remaining calibration constants via:

$$\hat{\beta}_Y = \frac{< YZ >}{< XZ >}$$

$$\hat{\beta}_Z = \frac{< YZ >}{< XY >}.$$

Here <> stands for a long-term average. Finally, we obtain the triple collocation estimates of the variances of ε_i i = X, Y, Z , which we note $Var_{TC}(\varepsilon_i)$, from

$$Var_{TC}(\varepsilon_X) = < \left(X - \frac{Y}{\hat{\beta}_Y} \right) \left(X - \frac{Z}{\hat{\beta}_Z} \right) >$$

$$Var_{TC}(\varepsilon_Y) = < \left(\frac{Y}{\hat{\beta}_Y} - X \right) \left(\frac{Y}{\hat{\beta}_Y} - \frac{Z}{\hat{\beta}_Z} \right) >$$

$$Var_{TC}(\varepsilon_Z) = < \left(\frac{Z}{\hat{\beta}_Z} - X \right) \left(\frac{Z}{\hat{\beta}_Z} - \frac{Y}{\hat{\beta}_Y} \right) > .$$

The square-root of the estimated error variances are the triple collocation estimates of the RMSE. Since GLDAS was taken as the reference data set, all estimates are given in GLDAS climatology, but they can be easily converted to another reference data set by multiplication with the appropriate calibration constant.

It should be noted that in order for these estimates to be consistent, all the assumptions of the triple collocation error model should hold. This is the case for the data sets used in this study, since no two of them use common input data or observations that could produce significantly correlated errors. Finally, it is important to remark that since the triple collocation study is based on deviations from the mean seasonal cycle, the estimates obtained represent only the errors in the anomalies of the soil moisture time series and therefore they do not provide any insight into errors in the mean season cycle or bias in the original time series.

4.3. Standardized Precipitation Index (SPI) and extremes definition

The Standardized Precipitation Index (SPI) was designed by [8] in order to monitor the water supply conditions of a particular region. Its simplicity and versatility are given by its dependence with only one variable, the precipitation, and the possibility to be calculated on any timescale. Moreover, the frequencies of the extreme and severe droughts classifications for any location and timescale are consistent [9]. In this paper, SPI is computed monthly. We defined an hydrological extreme in an area if Abs(SPI) > 2.

Therefore, we decided to use the SPI as an objective measurement of precipitation anomalies in order to define extreme conditions of water supply during the analyzed period. The NMS of Argentina operationally provides this index for different scales, considering the precipitation distribution of 1961-2000 as the reference interval (please referred to http://www.smn.gov.ar/serviciosclimaticos/). The SPI categories scale is detailed on Figures 7-11 of the Results section.

5. RESULTS

5.1. Preliminary analysis

As a preliminary analysis, we checked the consistency between product SM values and available in situ data. Although in situ data consist of only one point and therefore has limited representativeness, this first check is relevant to delineate the following operational evaluations strategies. Results are shown in Figure 2.

Figure 2. Direct comparison between SMOS, ASCAT and GLDAS SM estimations and in situ SM measurements.

Form the data, we can see that: (1) the correlation between satellite products and in situ data are relatively low, while GLDAS correlation is high; (2) satellite products present very different dynamic ranges, maximum and minimums and (3) GLDAS present only a systematic overestimation, which seem to be constant along all the SM range.

From these observations we can extract two preliminary results. First, GLDAS seem to be a good SM benchmark for this area and second, a comparison of absolute values of SM is not a convenient way to analyze satellite product performance, since products and in situ data present different dynamic ranges, maximums and minimums.

5.2. Spatial anomalies analysis

Since satellite products absolute SM estimations presented a low performance when compared with in situ SM data, it is relevant to compute SM estimations as defined in (**4.1**). Anomalies so defined have the potential to follow in situ SM anomalies, which can be very useful to several end user applications. Figure 3 shows an example of Austral Winter standardized spatial anomalies for both products and GLDAS for the 2010 period.

Figure 3. Product spatial anomalies of SMOS, ASCAT and GLDAS SM values (Austral Winter June 2010 – September 2010).

As seen, although the performance of absolute values is low, all spatial anomalies present high correlation among them (see Table 1). More important, spatial anomalies present the typical east-west SM gradient of the study area. This indicates that although satellite products and GLDAS present different dynamic ranges and sensitivities, they all carry some information about Pampas Plain SM spatial pattern. Moreover, this information is consistent with available macro meteorological information, which is specifically modeled by GLDAS and reproduced (to some degree) by satellite based products. This correlation between products and LSM (2nd and 3rd row of Table 1) is particularly relevant, since satellite based products do not take as input any meteorological data.

	Correlation	p-value
SMOS vs. ASCAT	0.879	< 0.01
ASCAT vs. GLDAS	0.789	< 0.01
SMOS vs. GLDAS	0.772	< 0.01

Table 1. Correlation between product anomalies.

5.3. Temporal anomalies analysis

The behavior of the temporal anomalies as defined in (**4.2**) around the site in which in situ SM data is available is presented in Figure 4.

Figure 4. SM temporal anomalies in the first row. SM absolute values in the second row. Precipitation stations close to Sol Negro site in the third row. Climatology for SMOS, ASCAT, GLDAS and in situ measurements in the fourth row. The period was constrained to the time period were in situ measurements were available (September 12 – January 14).

As seen, in the only site where comparisons with in situ measurements were possible, the temporal trend of SM temporal anomalies in general follows in situ measurements (first row). Moreover, SM temporal anomalies are sensitive to major precipitation events in the area (third row). On the contrary, absolute SM values present medium to large deviations from in situ measurements. The reasons of these deviations can be several, but a clue is provided by the temporal behavior of the climatology. In situ SM climatology presents low annual variations for this area, while ASCAT satellite product climatology presents strong annual variations, with minimums in winter and maximums in summer.

In summary, absolute satellite based SM estimation present strong discrepancies (dynamic ranges, variability, sensitivity to precipitations, seasonal behavior, others) among them and with in situ measurements. Nevertheless, SM spatial anomalies are quite similar (they show good correlation among them) and therefore worthy of being analyzed using an advanced technique as Triple Collocation.

5.4. Triple Collocation (TC) analysis

TC is able to estimate the error between real SM anomalies and satellite SM anomalies given a triplet of SM anomalies. Triple collocation results are summarized in Figure 5 and Table 2. Figure 5 shows three maps of the TC error estimations for each pixel and each product. As seen, ASCAT and SMOS present similar spatial distributions of overall TC errors, while GLDAS present more spatially homogeneous results. Larger errors in ASCAT seem to be located in areas of large biomass (crops), while SMOS errors are mainly located in coastal areas.

Figure 5. Overall TC error estimation for SMOS, ASCAT and GLDAS.

Table 2 summarizes the mains statistics of the TC analysis. It can be seen that the mean value of the error is very similar for all the three products for this area and the time period analyzed. This implies that the error between true SM anomalies and SMOS and ASCAT SM anomalies are similar. These results can be further visualized in Figure 6.

	GLDAS	ASCAT	SMOS
Mean	0.0273	0.0238	0.0270
Median	0.0268	0.0221	0.0231
SD	0.0052	0.0226	0.0473

Table 2. Mean, median and SD of overall TC estimates

Figure 6 shows a map of the satellite product that presents the lower TC error estimate. A pixel is assigned to a given product if TC_1 - TC_2 > threshold, where the threshold was selected as 0.002. As seen in the figure, the vast majority of the area is labeled as "Tie", indicating very similar TC error estimates for both products and also, very similar errors between true SM anomalies and satellite SM anomalies.

Figure 6. Map of the product which presents the minimum TC error estimation (errors are considered the same if $TC_1 - TC_2 < 0.002$).

From this analysis, it can be seen that the mean value of the TC error is very similar for all the products. Moreover, repeating this analysis for different time periods, seasons and landcover selections produce different results of TC error estimates (results not shown), with no definite best product. Therefore, if we seek an answer to which product best represents spatiotemporal SM patterns in this area and time period, TC analysis does not provide a conclusive answer.

Since standard metrics (anomalies analysis and TC error estimation) produce positive but inconclusive evidence, to evaluate product performance we propose an extreme event-detection analysis based on anomalies of the Standardized Precipitation Index (SPI).

5.5. SPI Extreme events analysis

Standardized Precipitation Index (SPI) is commonly used as an excess/shortage soil water indicator in areas where precipitation data is available, although in situ SM data may be not. As stated in the methodology, SPI is computed monthly. The methodology proposed is based on the analysis of the extremes defined by SPI. We defined an hydrological extreme in an area if Abs(SPI) > 2. This operational definition has two advantages. First, although the real values of SM and SPI are not generally correlated, when such an extreme conditions exist, extremes values of SM are generally observed [9]. Second, this definition has the added value of being closely related to several end-user requirements, which are mainly interested in extreme events associated with extremes in precipitation.

Before proceeding with the analysis, it is relevant to address the expected SM spatial structure of the events, since by definition SPI extremes are relatively large (of the order of 10^6 Ha). At these spatial scales, positive extremes does not imply uniformly wetter areas, since in this flat plain, the water enters the system mainly by precipitation, which is spatially heterogeneous [10]. This implies that a positive extreme will be seen as an increase in SM values, but not necessarily a significant increase in mean SM values. On the contrary, negative extremes, characterized by the uninterrupted reduction of precipitation, will be more spatially homogeneous, since the main forcing that extracts water from the system is the evapotranspiration, which at these scales depends mainly on sun total irradiation.

Using these definitions, five extreme events were identified in the four year time series. These events as seen by the SPI and the SM values for the whole time series (left boxplot) and the extreme month for the area of the event (right boxplot) for GLDAS, ASCAT and SMOS are presented in Figures 7-11. Each event will be analyzed independently.

5.4.1. Event #1: April 2010 (Figure 7).

Figure 7. SPI anomalies as seen by SPI, ASCAT, SMOS and GLDAS. April 2010 event.

Dry anomaly: No significant differences are observed between the boxplots of the event compared to the ones of the complete time series (median, quartiles). Moreover, a slightly increase in ASCAT SM values are observed.

The lack of sensitivity for this particular event can be related to several facts other than product performance. First, the event is spatially small, which is usually related to relatively large errors related to precipitation interpolation. Second, in April (Austral Autumn), main crop (soybean) is at its maximum biomass. Therefore, vegetation attenuation correction of satellite based estimations is critical in this period of the year.

5.4.2. Event #2: January 2011 (Figure 8).

Figure 8. SPI anomalies as seen by SPI, ASCAT, SMOS and GLDAS. Jan 2011 event.

Wet anomaly: Significant increases are observed between the boxplots of the event compared to the one of the complete time series for ASCAT (median from 0.12 m^3/m^3 to 0.15 m^3/m^3, 3rd quartile from 0.17 m^3/m^3 to 0.24 m^3/m^3 and upper whisker from 0.31 m^3/m^3 to 0.42 m^3/m^3). No significant differences are observed for GLDAS and SMOS.

The event is medium sized and occurred during Austral Summer (relatively high biomass). Boxplots show that some pixels inside the area show an increase of SM values, which corresponds to more heterogeneous SM values inside the area of the event. This is consistent with the expected behavior of the SM spatial pattern during a wet event as explained before.

5.4.3. Event #3: December 2011 (Figure 9).

Figure 9. SPI anomalies as seen by SPI, ASCAT, SMOS and GLDAS. December 2011 event.

Dry anomaly: Significant reductions are observed between the boxplots of the event compared to the one of the complete time series for all the products (median from 0.17 m^3/m^3 to 0.11 m^3/m^3 in GLDAS, from 0.17 m^3/m^3 to 0.10 m^3/m^3 in ASCAT and from 0.16 m^3/m^3 to 0.09 m^3/m^3 in SMOS. Similar decreases are observed in the 1st and 3rd quartile and upper whiskers for all products.

This event has a large size and occurred during Austral Summer (relatively high biomass). Boxplots show that the majority of pixels inside the area decrease their SM values, which corresponds to a less heterogeneous SM values inside the area of the event. This is consistent with the expected behavior of the SM spatial pattern during a dry event as explained before.

5.4.4. Event #4: February 2012 (Figure 10).

Figure 10. SPI anomalies as seen by SPI, ASCAT, SMOS and GLDAS. February 2012 event.

Wet anomaly: No significant differences are observed between the boxplots of the event compared to the one of the complete time series.

This event corresponds to two spatially disjoint events. The east event is located over Parana River Delta, for which SM estimations are not available (flagged in the products). Finally, the event occurs in Austral Summer (high biomass)

5.4.5. Event #5: August 2012 (Figure 11).

Figure 11. SPI anomalies as seen by SPI, ASCAT, SMOS and GLDAS. August 2012 event.

Wet anomaly: Significant increases are observed between the boxplots of the event compared to the one of the complete time series for all the products (median, 3rd quartile and upper whiskers).

This event has a large size and occurs in Austral Winter (low values of biomass). Boxplots show several pixels that increased their SM values, which corresponds to more heterogeneous SM values inside the area of the event. This is consistent with the expected behavior of the SM spatial pattern during a wet event as explained before.

6. DISCUSSION

In this paper, a first analysis of the performance of two candidate soil moisture products (ASCAT and SMOS) over Argentine Pampas Plain was presented. The overall performance metric was defined as the ability to monitor SM spatiotemporal patterns. Since product absolute SM values presented large discrepancies, our approach to measure this ability consisted in using four different metrics: SM spatial anomalies analysis, SM temporal anomalies analysis, TC error estimation analysis and SPI extreme events analysis.

6.1. SM spatial anomalies analysis

Spatial anomalies analysis was overall successful, since it showed that both satellite based products and GLDAS were able to reproduce similar large scale macro-meteorological SM patterns in the study area. This is observed in the good correlation among anomalies (Table 1) and in the similarities between products and GLDAS. The satellite derived spatial anomalies present the typical east-west SM gradient of the study area, which is related to specific precipitation and evapotranspiration patterns (see Figure 1, right). This indicates that satellite products carry valuable information about overall Pampas Plain SM spatial pattern. This correlation between products and expected SM patterns is important, since satellite-based products do not take as input precipitation or evapotranspiration data.

6.2. SM temporal anomalies analysis

It is relevant to mention that in situ SM climatology presented low annual variations for Sol Negro Station (in situ SM available), while ASCAT satellite product climatology presented strong annual variations, with minimums on winter and maximums in summer. Although there is no sufficient evidence to test this hypothesis, it is probable that this artifact is related to incomplete vegetation attenuation correction due to C band limitations.

6.3. TC error estimation analysis

From the TC analysis it was possible to generate a map of the overall TC error estimations for the study area (Figure 5). These results were summarized in Table 2. In general terms, larger errors in ASCAT seem to be located in areas of large biomass (crops), while SMOS errors are mainly located in coastal areas. The first also seems to be related to incomplete vegetation attenuation correction, which is particularly relevant at C band, while the second is probably due to geo-location errors associated with SMOS data generation strategy [5]. Nevertheless, considering a minimal error difference as significant, in most of the study area the products are characterized by the same TC error estimates (see Figure 6).

6.4. SPI extreme events analysis

Extreme results are probably the most relevant result of this paper. In this analysis, it was shown that products are able to follow some SPI extremes (ASCAT: 3 of 5, SMOS: 2 of 5) present in the four year time series available. For the extremes that were not detected, several explanations were presented. First, arguments related to SPI overall quality for small areas, in which spatial interpolation of precipitation is critical, were discussed (event #1). Second, considerations about seasonality were discussed in the context of vegetation biomass. Indeed, vegetation attenuation correction is the main issue of several satellite based SM products. Since Pampas Plain is a cropland, vegetation cycle of the area are synchronous and peaks at Austral summer, leading to larger biomass, larger attenuations and more important corrections. Due to operational wavelength and physical constraints, this correction can be the key factor that controls product performance. This is therefore more important at C band (ASCAT) that at L band (SMOS).

In summary, satellite based products were able to follow extreme hydrological events when biomass was low and more homogeneous (Austral winter, event #5) or biomass was moderate to high but the event was strong and spatially large (events #2 and #3).

7. CONCLUSIONS

In this paper, an operational evaluation strategy for two candidates satellite derived SM products was presented. The strategy is operational since it involves the analysis of data which are satellite derived or common in most areas (like precipitations). It is an evaluation and not a validation since no in situ field experiment of the required size and instrumentation is available in the area, and therefore no proper

validation is possible. On the contrary, the proposed methodology relies in comparison of product SM metrics that show expected SM spatiotemporal patterns. These metrics were selected to overcome product limitations, and to be able to provide relevant information to the end user. In this context it was shown that: (1) both ASCAT and SMOS spatial anomalies data are able to reproduce the expected SM spatial patterns, (2) both ASCAT and SMOS temporal anomalies are able to follow the measured in situ SM temporal anomalies and (3) both products were able to monitor large SPI extremes, at least in conditions where crop biomass was moderate to low.

8. ACKNOWLEDGMENTS

We want to specially thank Dr. Wade Crow for the triple collocation code and CONAE for in situ SM data.

9. REFERENCES

[1] Hain, C. R., W. T. Crow, J. R. Mecikalski, M. C. Anderson, and T. Holmes, "An intercomparison of available soil moisture estimates from thermal infrared and passive microwave remote sensing and land surface modeling", *J. Geophys. Res. 116*, American Geophysical Union, USA, pp. 1-18, 2012.

[2] INTA (Instituto Nacional de Tecnología Agropecuaria), "Cobertura del suelo de la República Argentina. Año 2006-2009.", http://inta.gob.ar/documentos/cobertura-del-suelo-de-la-republica-argentina.-ano-2006-2007-lccs-fao/ .

[3] Pántano, V. C. y Penalba, O. C., "Respuesta de la situación hídrica del suelo a la variabilidad temporal de la precipitación", XI Congreso Argentino de Meteorología (CONGREMET XI), Mendoza, Argentina, 2012.

[4] Wagner, W., Hahn, S., Kidd, R., Melzer, T., Bartalis, Z., Hasenauer, S., Figa-Saldaña, J., de Rosnay, P., Jann, A., Schneider, S., Komma, J., Kubu, G., Brugger, K., Aubrecht, C., Züger, J., Gangkofner, U., Kienberger, S., Brocca, L., Wang, Y., Blöschl, G., Eitzinger, J., Steinnocher, K., Zeil, P., Rubel, F., 2013. The ASCAT Soil Moisture Product: A Review of its Specifications, Validation Results, and Emerging Applications. Meteorologische Zeitschrift, 22(1):5–33.

[5] Kerr, Y. H., Waldteufel, P., Richaume, P., Wigneron, J. P., Ferrazzoli, P., Mahmoodi, A., Al Bitar, A., Cabot, F., Gruhier, C., Juglea, S. E., Leroux, D., Mialon, A. and Delwart, S., "The SMOS Soil Moisture Retrieval Algorithm". *IEEE Transactions on Geoscience and Remote Sensing*, 50(5):1384–1403, 2012.

[6] http://www.conae.gob.ar

[7] Stoffelen, A., "Toward the true near-surface wind speed: Error modeling and calibration using triple collocation", *J. Geophys. Res.,* American Geophysical Union, USA, pp. 7755-7766, 1998.

[8] McKee, T. B., N. J. Doesken, and J. Kleist, 1993: The relationship of drought frequency and duration to time scales. Preprints, Eighth Conf. on Applied Climatology, Anaheim, CA, Amer. Meteor. Soc., 179–184.

[9] Hayes, M. J., Svoboda M. D., Wilhite D. A. and Vanyarkho O.V., 1999: Monitoring the 1996 Drought Using the Standarized Precipitation Index. BAMS, Vol.80, No.3, p. 429-438.

[10] C.M. Matsudo, P.V. Salio, Severe weather reports and proximity to deep convection over Northern Argentina, Atmospheric Research, Volume 100, Issue 4, June 2011, Pages 523-537, ISSN 0169-8095, http://dx.doi.org/10.1016/j.atmosres.2010.11.004.

Figures

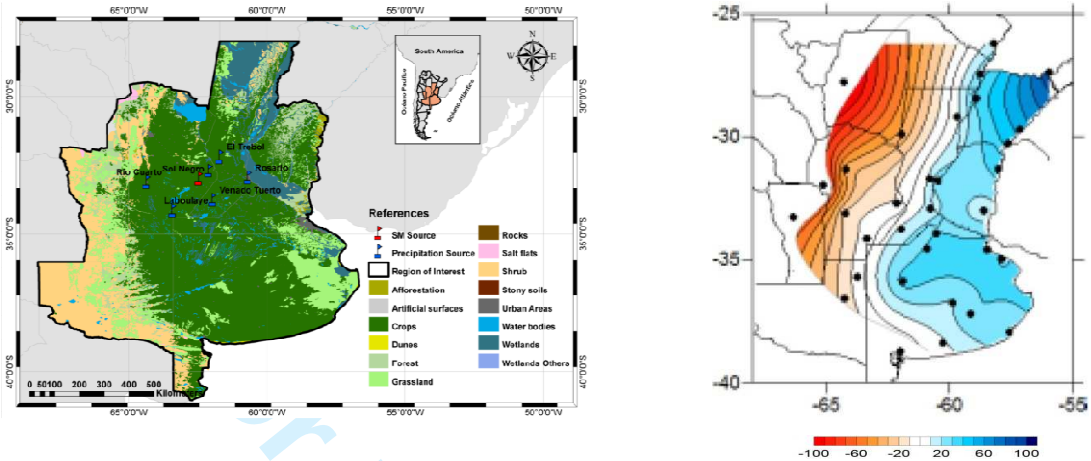

Figure 1. Study area. (left) Pampas Plains land cover categories (adapted from [1]) and (right) an example of the spatial distribution of the P-EP for the period 1970-2006 for the month of October (adapted from [2]).

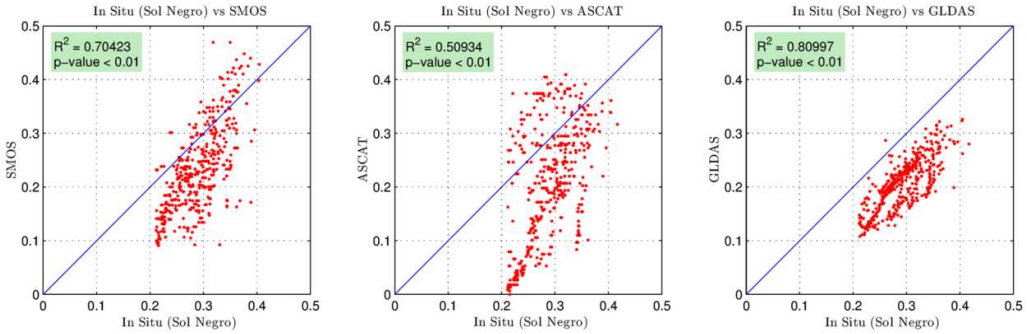

Figure 2. Direct comparison between SMOS, ASCAT and GLDAS SM estimations and in situ SM measurements.

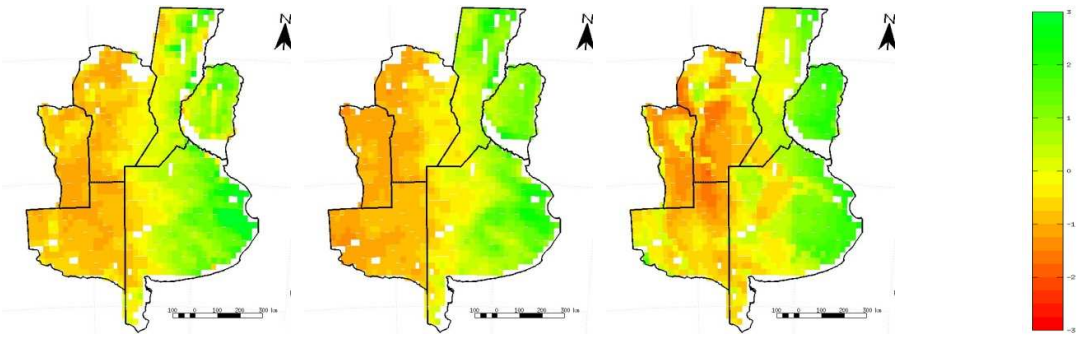

Figure 3. Product spatial anomalies of SMOS, ASCAT and GLDAS SM values (Austral Winter June 2010 – September 2010).

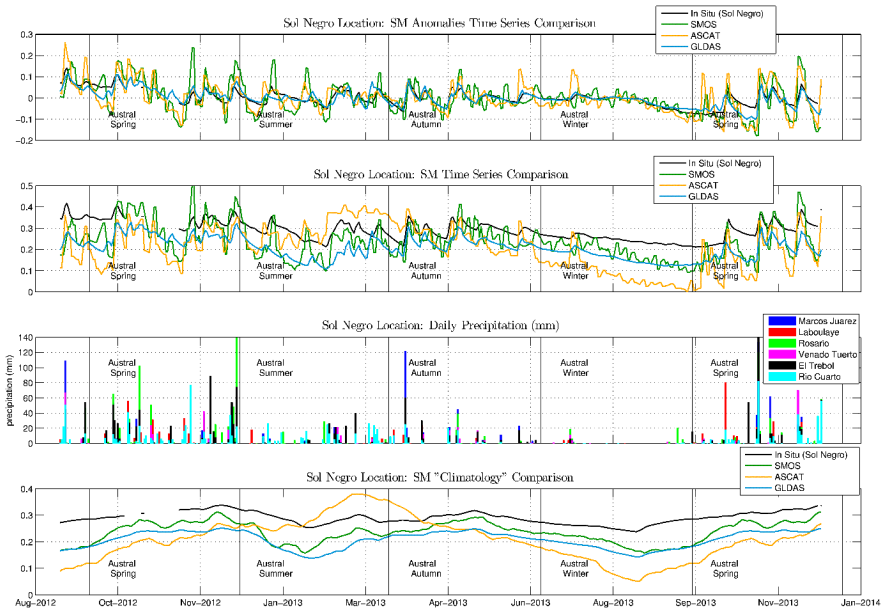

Figure 4. SM temporal anomalies in the first row. SM absolute values in the second row. Precipitation stations close to Sol Negro site in the third row. Climatology for SMOS, ASCAT, GLDAS and in situ measurements in the fourth row. The period was constrained to the time period were in situ measurements were available (September 12 – January 14).

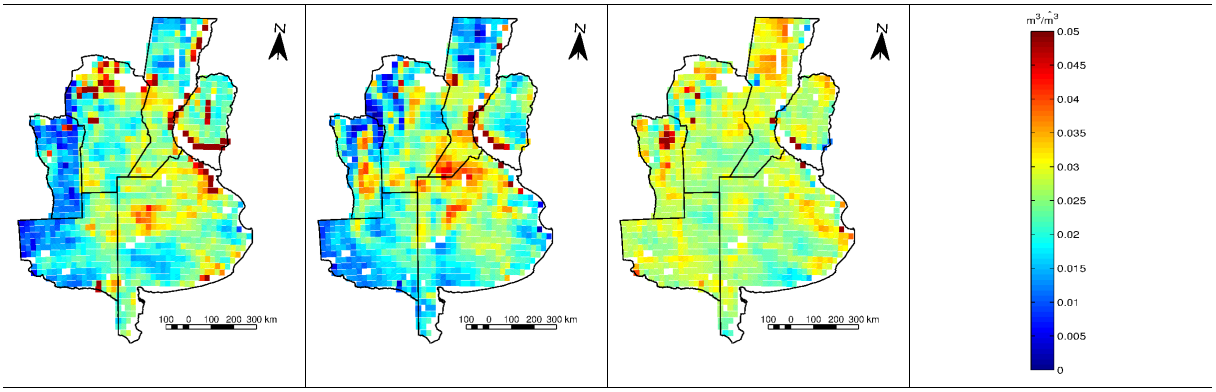

Figure 5. Overall TC error estimation for SMOS, ASCAT and GLDAS.

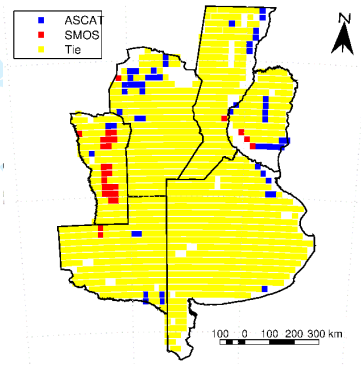

Figure 6. Map of the product which presents the minimum TC error estimation (errors are considered the same if $TC_1 - TC_2 < 0.002$).

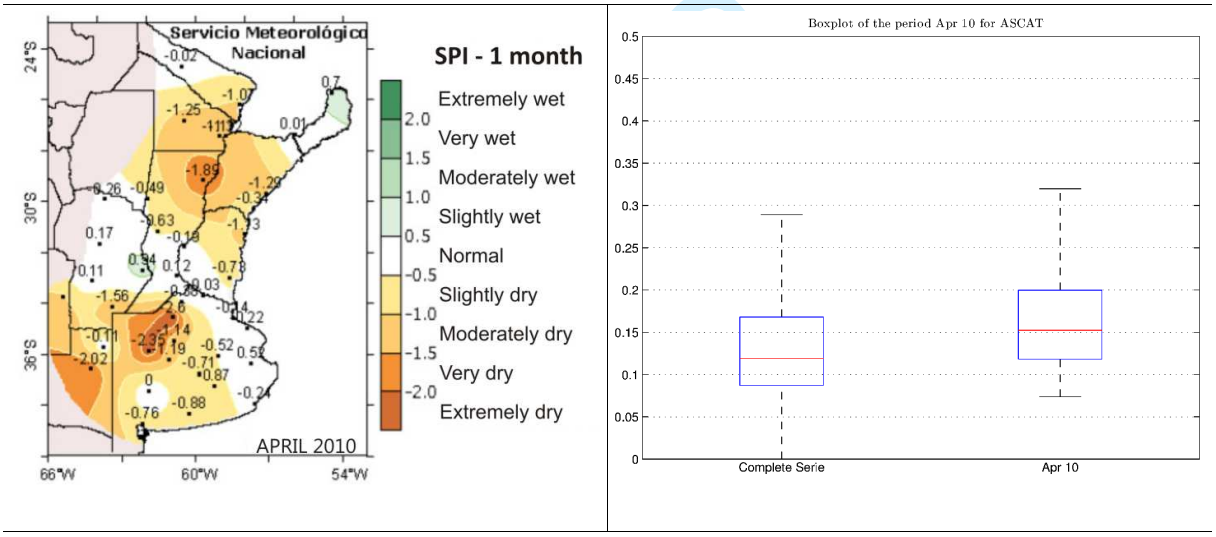

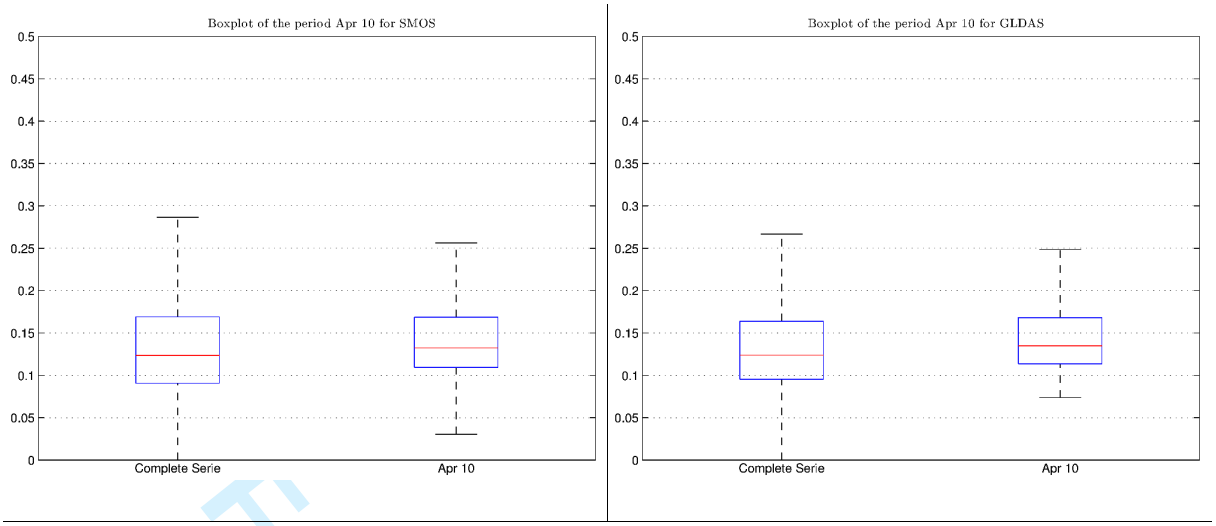

Figure 7. SPI anomalies as seen by SPI, ASCAT, SMOS and GLDAS. April 2010 event.

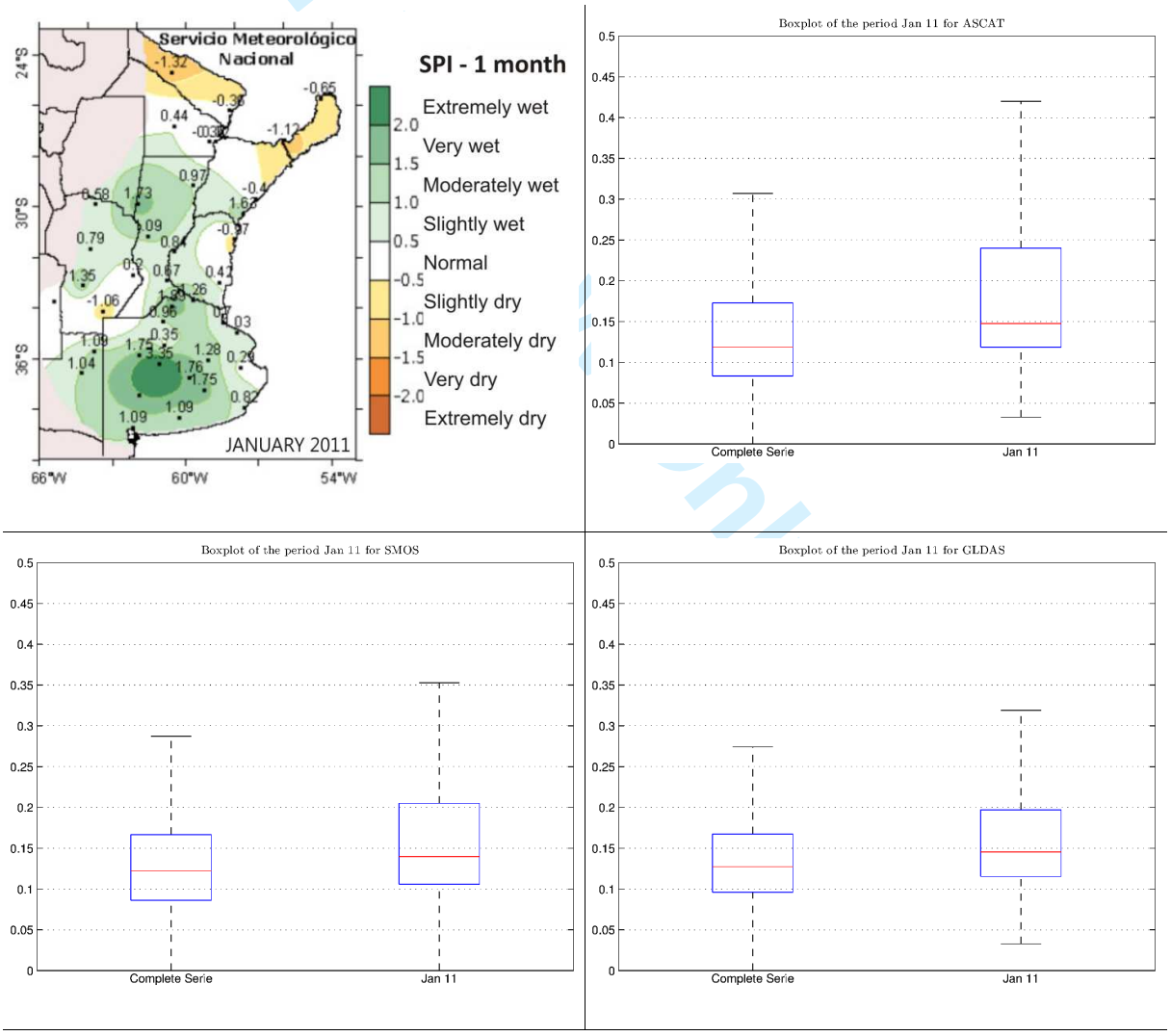

Figure 8. SPI anomalies as seen by SPI, ASCAT, SMOS and GLDAS. January 2011 event.

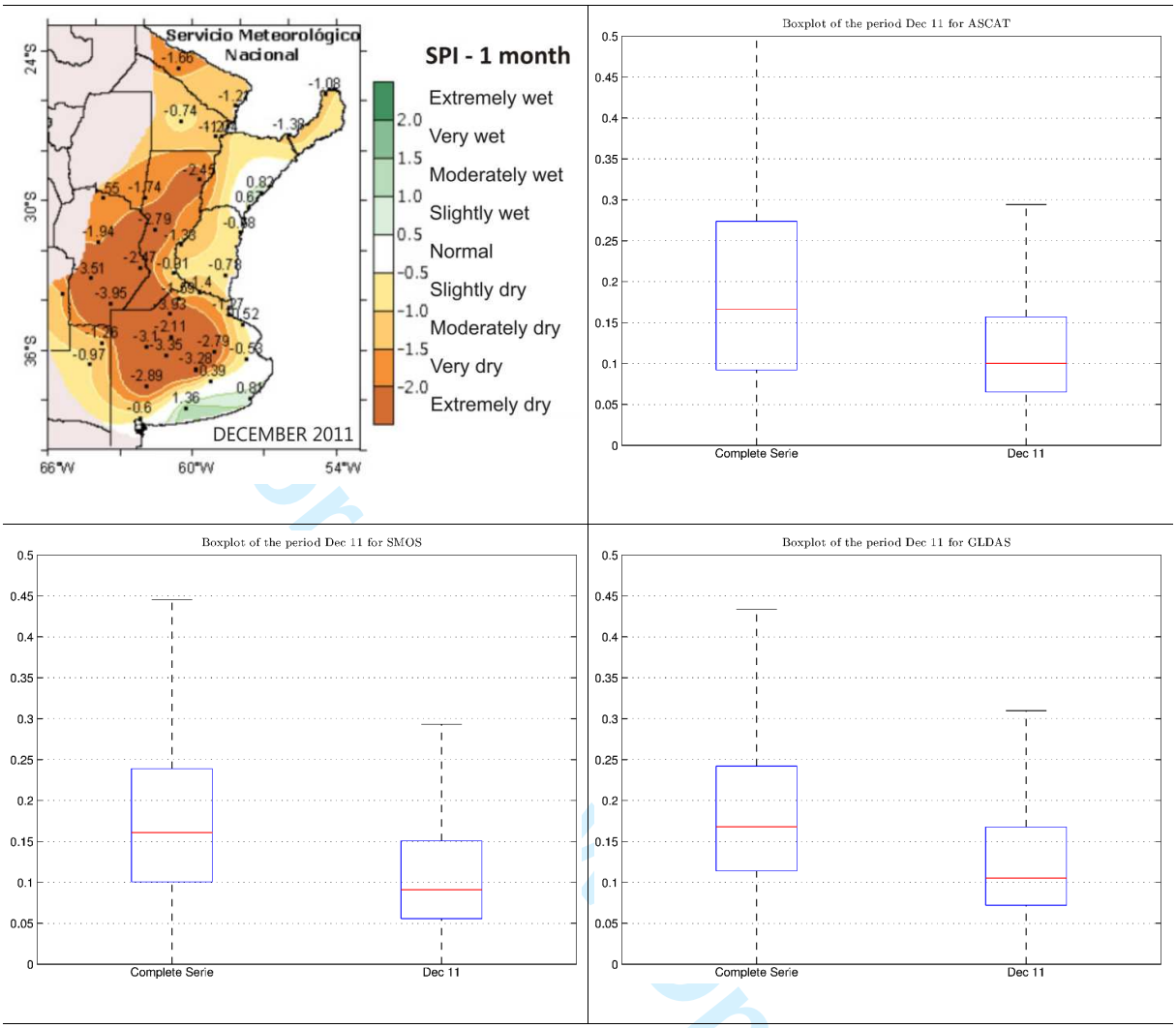

Figure 9. SPI anomalies as seen by SPI, ASCAT, SMOS and GLDAS. December 2011 event.

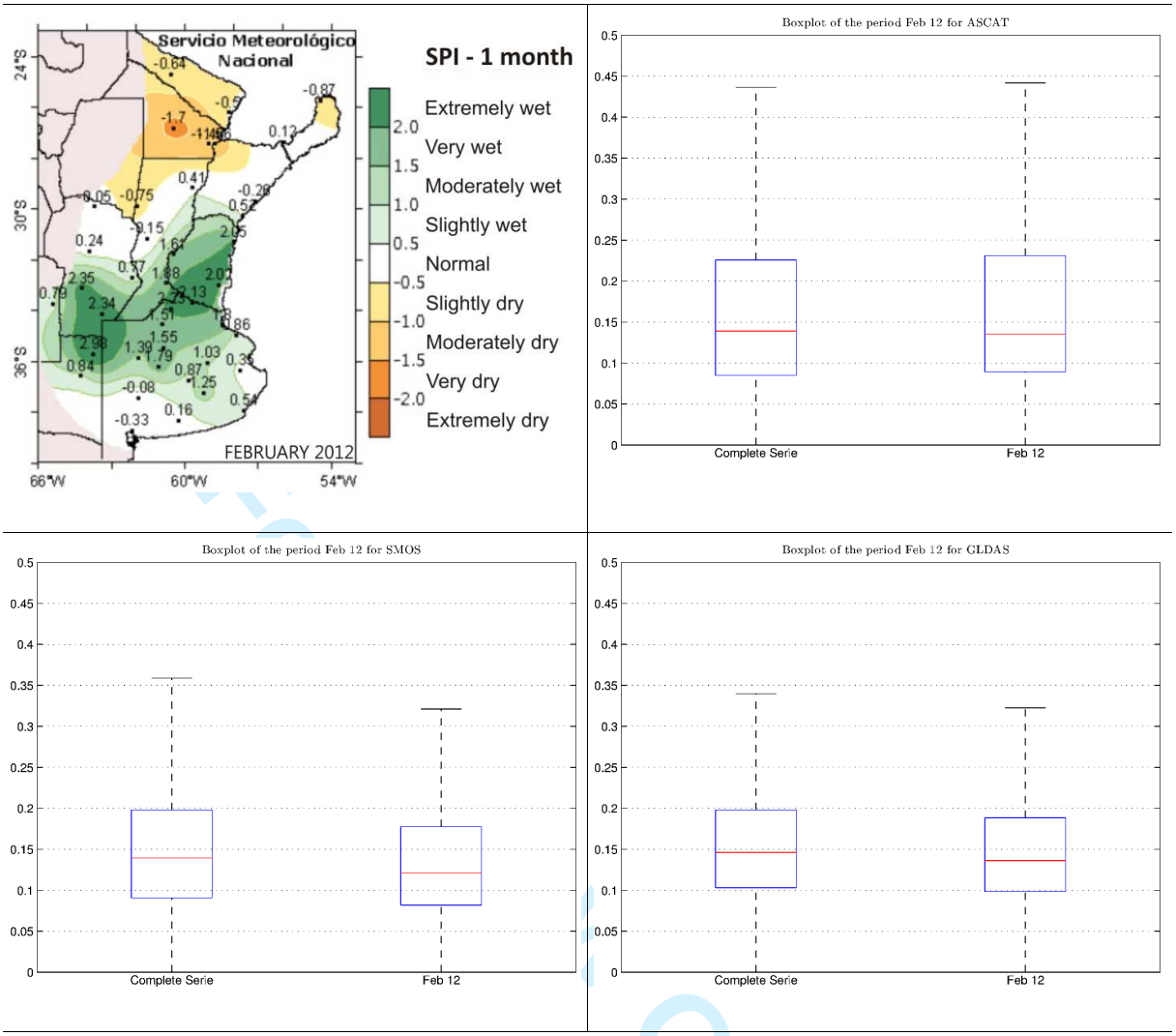

Figure 10. SPI anomalies as seen by SPI, ASCAT, SMOS and GLDAS. February 2012 event.

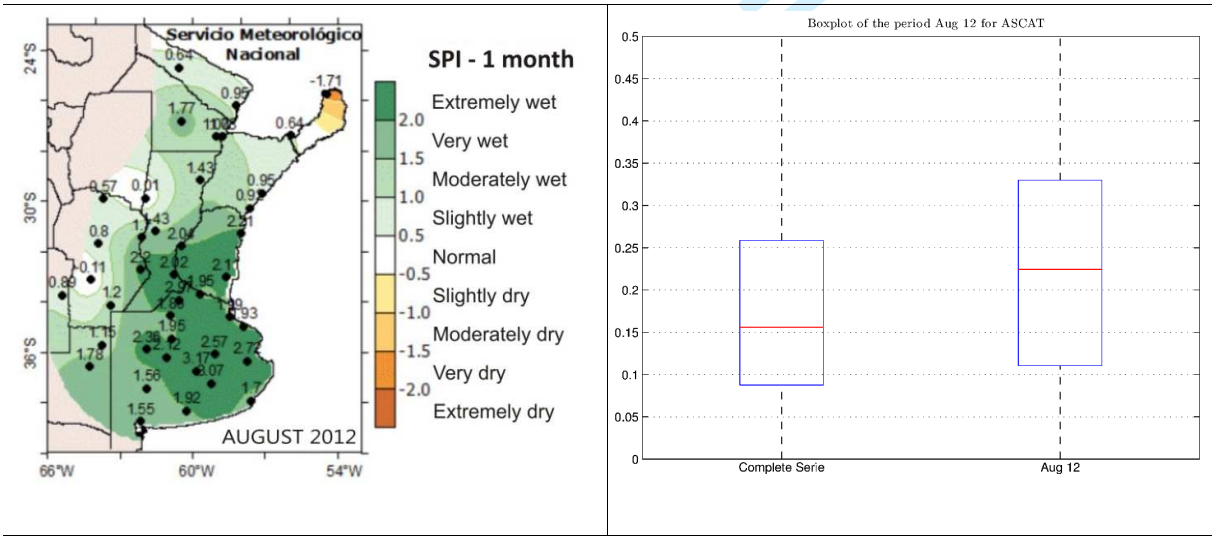

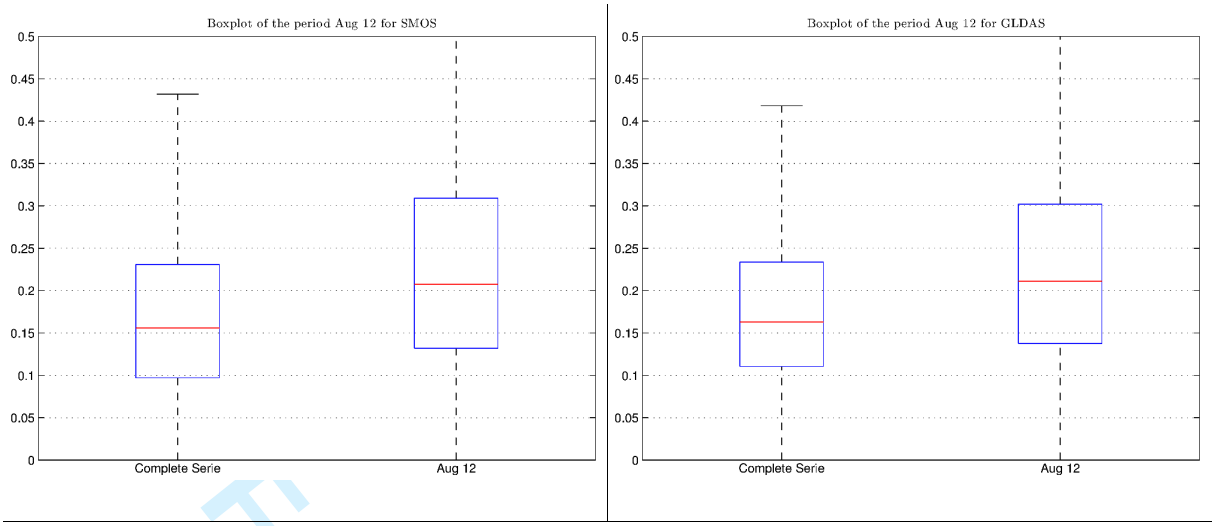

Figure 11. SPI anomalies as seen by SPI, ASCAT, SMOS and GLDAS. August 2012 event.